The American Journal of Pathology, Vol. 170, No. 2, February 2007

DOI: 10.2353/ajpath.2007.060676

Musculoskeletal Pathology

Overexpression of Rapsyn in Rat Muscle Increases Acetylcholine Receptor Levels in Chronic Experimental Autoimmune Myasthenia Gravis

Pilar Martínez-Martínez,*† Mario Losen,*† Hans Duimel,‡ Peter Frederik,‡ Frank Spaans,§ Peter Molenaar,¶ Angela Vincent,‖ and Marc H. De Baets*,**†

From the Department of Neurology, Research Institute Brain and Behaviour, and the Department of Pathology,‡ Electron Microscopy Unit, University of Maastricht, Maastricht, The Netherlands; European Graduate School of Neuroscience,† Maastricht, The Netherlands; the Departments of Clinical Neurophysiology§ and Neurology,** Maastricht University Hospital, Maastricht, The Netherlands; the Department of Molecular Cell Biology,¶ Neurophysiology Group, Leiden University Medical Centre, Leiden, The Netherlands; and the Neurosciences Group,‖ Weatherall Institute of Molecular Medicine, The John Radcliffe Hospital, Oxford, United Kingdom*

The primary autoantigen in myasthenia gravis, the acetylcholine receptor (AChR), is clustered and anchored in the postsynaptic membrane of the neuromuscular junction by rapsyn. Previously, we found that overexpression of rapsyn by cDNA transfection protects AChRs in rat muscles from antibody-mediated loss in passive transfer experimental autoimmune myasthenia gravis (EAMG). Here, we determined whether rapsyn overexpression can reduce or even reverse AChR loss in muscles that are already damaged by chronic EAMG, which mimics the human disease. Active immunization against purified AChR was performed in female Lewis rats. Rapsyn overexpression resulted in an increase in total muscle membrane AChR levels, with some AChR at neuromuscular junctions but much of it in extrasynaptic membrane regions. At the ultrastructural level, most endplates in rapsyn-treated chronic EAMG muscles showed increased damage to the postsynaptic membrane. Although rapsyn overexpression stabilized AChRs in intact or mildly damaged endplates, the rapsyn-induced increase of membrane AChR enhanced autoantibody binding and membrane damage in severe ongoing disease. Thus, these results show the complexity of synaptic stabilization of AChR during the autoantibody attack. They also indicate that the expression of receptor-associated proteins may determine the severity of autoimmune diseases caused by anti-receptor antibodies. ***(Am J Pathol 2007, 170:644–657; DOI: 10.2353/ajpath.2007.060676)***

The molecular organization of the neuromuscular junction (NMJ) is designed for optimal transmission of the signal from nerve to muscle (neuromuscular transmission), with nicotinic acetylcholine receptors (AChR) clustered at high density on the postsynaptic muscle membrane.[1] In myasthenia gravis (MG), the AChR is the main autoantigen, and the postsynaptic membrane of the NMJ is the target for antibody-induced damage. Anti-AChR antibodies are found in ~85% of MG patients. The antibodies cause loss of functional AChRs by cross-linking the receptors, leading to increased turnover of the AChR (antigenic modulation), by activating complement and leading to focal loss of the postsynaptic membrane folding, and/or by blocking the AChR ion channel.[2] Loss of functional AChRs compromises neuromuscular transmission, resulting in skeletal muscle weakness.

The high density and remarkable stability of the AChRs at the NMJ is dependent on rapsyn, a 43-kd membrane protein that is also essential for the formation of the postsynaptic apparatus.[3] The clustering of postsynaptic proteins during development is initiated by agrin, a neuronal protein that acts via a receptor complex including muscle-specific kinase.[4] Agrin triggers phosphorylation

Supported by the Prinses Beatrix Fonds (grant MAR03-0115), L'Association Française Contre les Myopathies, the European Community (quality of life and management of living resources project grant QLG3-CT-2001-00225), and the Dutch Scientific Organization (medical section grant no. 902-16-276 for the Bio-Rad TPLSM).

P.M.-M. and M.L. contributed equally to this work.

Accepted for publication October 31, 2006.

Address reprint requests to Dr. Pilar Martínez-Martínez or Dr. Marc H. De Baets, Department of Neurology, Research Institute Brain and Behaviour, University of Maastricht, P.O. Box 616, 6200 MD Maastricht, The Netherlands. E-mail: p.martinez@np.unimaas.nl and m.debaets@immuno.unimaas.nl.

of both muscle-specific kinase and AChR, resulting in the clustering and anchoring of preassembled AChR-rapsyn complexes to the cytoskeleton.[5] Rapsyn links the AChR to β-dystroglycan,[6] which in turn is linked to F-actin via utrophin.[7] Mice deficient in rapsyn die perinatally because the postsynaptic specialization of the NMJ fails to develop and respiratory paralysis occurs.[3] Mutations causing low expression of rapsyn in humans lead to a decreased AChR level and a simplified postsynaptic membrane folding.[8,9] Besides being essential for clustering, rapsyn metabolically stabilizes the AChR: cotransfection of rapsyn and AChR expression plasmids increases the half-life of AChR in cell lines,[10,11] and rapsyn also reduces antigenic modulation of AChRs in transfected fibroblasts when incubated with the anti-AChR monoclonal antibody (mAb) 35.[10]

Experimental autoimmune MG (EAMG) is an animal model that closely resembles clinical MG.[12] EAMG can be induced by passive transfer of MG patient sera or anti-AChR mAbs or by immunization with tAChR derived from *Torpedo* electric organ (chronic EAMG); the resulting antibodies against tAChR cross-react with muscle AChR in the immunized animal. Similar to MG, antigenic modulation and complement-mediated focal damage of the postsynaptic membrane are the main pathogenic mechanisms that lead to muscle weakness with impaired swallowing ability, hunched posture, drooping of the head, and limb weakness. Chronic EAMG is more similar to human MG than passive transfer EAMG because it models the continuous attack of autoantibodies throughout a long time period (>2 weeks); during this time the muscle may change the expression of postsynaptic proteins and complement regulatory proteins that reduce further damage to the endplate.

Age- and sex-dependent resistance to the induction of passive transfer and chronic EAMG has been observed in Lewis and Brown Norway rats.[13–16] Young rats, both male and female, are very susceptible to EAMG but progressively become resistant. In female rats, the resistance is incomplete because the induction of chronic EAMG in aged animals still results in 40 to 50% of AChR loss, albeit without clinical symptoms. Male rats develop a complete resistance to both passive transfer and chronic EAMG.[15] This resistance is not attributable to differences of the immune response or compensatory mechanisms such as increased expression of AChRs or complement modulatory proteins.[15–17] In fact, the postsynaptic membrane is intrinsically resistant to antibody-mediated degradation in aged animals of both strains.[14] In aged rats, rapsyn levels are increased relative to those of the AChRs, suggesting that rapsyn can make the AChR resistant to antibody-mediated degradation.[14] To investigate the therapeutic potential of increasing rapsyn expression, we used *in vivo* gene transfection and demonstrated protection against passive transfer EAMG,[18] with retained AChR and minimal ultrastructural damage at the endplates of rapsyn-transfected muscles.

These observations suggest that rapsyn expression might also be able to reverse the deficits in ongoing EAMG. Here, we have tested the effect of rapsyn overexpression in rat muscle during chronic EAMG. The results indicate a more complex relationship between rapsyn expression and AChR numbers than anticipated because rapsyn increased membrane AChR numbers but at the same time enhanced the damage of the postsynaptic membrane in damaged endplates and in the continuous presence of autoantibodies.

Materials and Methods

Animals

Six-week-old female Lewis rats were obtained from the Department of Experimental Animal Services, University of Maastricht, Maastricht, The Netherlands, with permission of the Committee on Animal Welfare, according to Dutch governmental rules. For immunization, *in vivo* electroporation and electromyography measurements, the animals were anesthetized with 3% isoflurane in air, supplied over a cylindrical cap held over the head. The animals were euthanized by CO_2/air inhalation and subsequent cervical dislocation.

Induction of Chronic EAMG

The animals were immunized at the base of the tail with 20 μg of tAChR in 0.1 ml of phosphate-buffered saline (PBS) emulsified in an equal amount of complete Freund's adjuvant (Difco Laboratories, Detroit, MI).[12] Blood samples were taken from the tip of the tail weekly, and in addition, the weight of the animals were recorded. After 5 weeks the rats were clinically scored, anesthetized for electropermeabilization, and euthanized 2 weeks later.

Electropermeabilization

The expression plasmid pcDNA1.1-rapsyn[18] was prepared for electropermeabilization with the Qiagen Maxiprep (Qiagen Benelux B.V., Venlo, The Netherlands), according to the manufacturer's manual, and finally dissolved in 0.9% NaCl at a concentration of 2 μg of DNA/μl. Seventy-five μl (2 μg/μl) of pcDNA-rapsyn was injected in aliquots at seven to eight sites equally spread over the muscle and electropermeabilized in the tibialis anterior[19] with the same parameters as previously described[18] using the Electro Square Porator ECM 830 (BTX, San Diego, CA).

Clinical Scoring

The severity of clinical signs of disease in EAMG was scored by measuring muscular weakness. The animals' muscle strength was assessed by their ability to grasp and lift repeatedly a 300-g rack from the table while suspended manually by the base of the tail for 30 seconds.[15,16,20] Clinical scoring was based on the presence of tremor, hunched posture, muscle strength, and signs of fatigue. Disease severity was expressed as follows: 0, no obvious abnormalities; +, no abnormalities before

testing but reduced strength at the end; ++, clinical signs present before testing, ie, tremor, head down, hunched posture, weak grip; +++, severe clinical signs present before testing, no grip, moribund.[12]

Electromyography

Decrement of compound muscle action potential was measured in the tibialis anterior muscles of three control and three EAMG rats as previously described.[18] To detect a decrementing response, a series of eight supramaximal stimuli were given at 3 Hz. Stimulus duration was 0.2 ms. This test was repeated 10 minutes after injection of 3 to 6 μg of curare.[21] The test was considered positive for decrement when both the amplitude and the area of the negative peak of the compound muscle action potential showed a decrease of at least 10%.[22] To demonstrate reproducibility, at least three recordings were made of all investigated muscles. During the measurements, skin temperature was kept between 35°C and 37°C by means of a heating pad. All electromyography studies were performed by the same investigator (F.S.).

Measurement of Serum Anti-Rat AChR Antibody Titers

Serum was obtained before immunization and afterward weekly up to the euthanasia. Anti-rat AChR serum antibodies were measured using crude extract of denervated rat muscle AChR: 100 μl of rat AChR extract (~5 nmol/L) were labeled with an excess of ^{125}I-α-BT (5.55 TBq/mmol; GE Health Care) and incubated with 5 μl of rat serum at 4°C overnight. The resulting complexes were precipitated by the addition of 100 μl of goat anti-rat Ig, 4 hours incubation, and centrifugation at 15,000 $\times$ *g* for 5 minutes. The pellets were washed three times in PBS with 0.5% Triton X-100 and measured in a gamma counter. Titers were corrected for the background of normal rat serum. The antibody titer was expressed as mol of α-BT binding sites/L.

Immunohistochemical Staining

Isolated tibialis anterior muscles of three control and six EAMG animals were frozen in melting isopentane. Cryosections of 10 μm were dried, fixed in acetone at 4°C for 10 minutes, dried, and blocked for 20 minutes with PBSA (phosphate-buffered saline with 2% bovine serum albumin). Sections were incubated with the following antibodies: mouse anti-rapsyn mAb 1234 (1/500 in PBSA; Affinity Bioreagents, Golden, CO)[23]; mAb 2A1 against rat C5b-9 (membrane attack complex, 1/100 in PBSA; kindly provided by W.G. Couser, University of Washington, Seattle, WA); rabbit anti-vesicular acetylcholine transporter (VAChT, 1/500 in PBSA; Phoenix Pharmaceuticals, Belmont, CA); mouse anti-utrophin mAb MANCHO 7 (1/100 in PBSA; kindly provided by Prof. G.E. Morris, North East Wales Institute, Wrexham, UK),[24] and Alexa 594-conjugated α-bungarotoxin (Alexa 594-α-BT; 1/300 in PBSA; Molecular Probes, Leiden, The Netherlands) overnight at 4°C and finally washed with PBS with 0.05% Triton X-100. Subsequently, the sections were incubated for 1.5 hours at room temperature with the corresponding secondary antibodies: biotinylated donkey anti-mouse Ig (1/400, minimal cross-reaction with rat IgG; Jackson Immunoresearch, West Grove, PA) or Alexa 350-conjugated goat anti-rabbit (1/100; Molecular Probes). After washing as described above, the biotinylated antibodies were stained for 1.5 hours at room temperature with Alexa 488-streptavidin (1/2000; Molecular Probes). Coverslips were mounted with 0.2 mol/L Tris, pH 8, with 80% (v/v) glycerol.

Quantitative Immunofluorescence Analysis

Pictures of muscle sections were taken using a Provis AX70 fluorescent microscope (Olympus, Hamburg, Germany) with a digital camera (U-CMAD-2; Olympus) and the AnalySIS software (Soft Imaging Systems, Münster, Germany). Sections triple stained for VAChT, rapsyn, or utrophin, and AChR were photographed using filters for Alexa 350, fluorescein isothiocyanate, and Alexa 594 fluorescence. A fivefold reduced concentration of primary antibodies and α-BT did not result in a weaker staining, therefore they did not limit staining intensity. Pictures were analyzed using the ImageJ software (version 1.33n; *http://rsb.info.nih.gov/ij*). Endplate areas were identified by the presynaptic staining of VAChT and the mean intensity of VAChT, rapsyn, or utrophin, and AChR staining was measured in the corresponding area. The ratios of AChR/VAChT, rapsyn/VAChT, and utrophin/VAChT were calculated for more than 200 endplates per muscle as a relative measure for the postsynaptic rapsyn, utrophin, and AChR concentration. All sections were stained and processed in parallel to avoid interassay variations.

Two-Photon Laser-Scanning Microscopy

High-resolution pictures of endplates were taken using a two-photon laser scanning microscope setup as previously described.[25] A 40$\times$ oil immersion objective with a numerical aperture of 1.0 was used. Further magnification was achieved by optical zoom (4$\times$) of the scan head. Picture stacks with an axial resolution of 0.15 μm and a lateral resolution of 0.13 μm were taken using photomultipliers accepting wavelengths of 470 to 500 nm, 520 to 560 nm, and more than 560 nm. To remove background, each image was filtered applying the Kalman filtering procedure on two subsequent images. For projection of the images, the ImageJ software was used.

Muscle Membrane Extracts

Tibialis anterior muscles were minced and homogenized with an Ultra-Turrax (3 times for 30 seconds at 4°C) in 10 ml of buffer A (PBS, 10 mmol/L ethylenediaminetetraacetic acid, 10 mmol/L NaN_3, 10 mmol/L iodoacetamide, and 1 mmol/L phenylmethyl sulfonyl fluoride). The homoge-

nate was centrifuged (22,100 × *g*, 30 minutes), and the resulting pellet was resuspended in 2.5 ml of buffer B (buffer A with an additional 0.5% Triton X-100). Extraction was performed for 1 hour at 4°C on a reciprocal shaker followed by centrifugation (22,100 × *g*, 30 minutes). The AChR was measured immediately by radioimmunoassay.

Measurement of Total Muscle AChR by Radioimmunoassay

The AChR concentrations of isolated tibialis anterior muscles from five control and 10 EAMG rats were measured as described previously.[18] The AChR concentration per g of fresh muscle weight was calculated in fmol/g ± SD, and differences between concentrations are presented in percentage ± SE of the difference of the means. Differences between samples were analyzed using a two-sided *t*-test (paired differences were used for comparison of rapsyn-treated versus control in the same experimental group).

Measurement of Antibody-AChR Complexes and Rapsyn-AChR Aggregates by Radioimmunoassay

For measurement of antibody-AChR complexes formed *in vivo* in EAMG,[26,27] triplicate aliquots of 200 μl were taken from the muscle membrane extracts, and each aliquot was incubated with an excess (25 fmol) of ^{125}I-α-BT and 1 μl of normal rat serum. After overnight incubation at 4°C, the samples were processed using the aforementioned radioimmunoassay protocol for total muscle AChR. A similar assay was used to test whether rapsyn increased AChR crosslinking in membrane extracts independent of autoantibodies. For measurement of rapsyn-AChR aggregates, a limited amount of rat anti-rat-AChR antibodies (equivalent to 64 fmol of α-BT binding sites) was added to triplicate 200-μl aliquots of the muscle membrane extracts of untreated and rapsyn-treated control rats. In this way, if there were an aggregate of, for example, three molecules of AChR complexed with rapsyn, the binding of one IgG molecule to the AChR would cause the whole aggregate to be precipitated, increasing the radioactivity threefold compared with precipitation in the absence of aggregates (Figure 3A). A second set of triplicate aliquots was incubated without added anti-AChR antibodies and served as control. After overnight incubation at 4°C, the samples with or without added antibody were processed using the aforementioned radioimmunoassay protocol for total muscle AChR.

Electron Microscopy

Electron micrographs were taken from endplates of the tibialis anterior muscles of three EAMG rats and three control rats with unilateral rapsyn treatment as previously described.[18] In brief, anesthetized rats were transcardially perfused with Tyrode solution followed by 2.5% glutaraldehyde fixation buffer. The tibialis anterior muscles were postfixed with 1% osmium tetroxide, dehydrated through a graded ethanol series, and embedded in epoxy resin. Ultra-thin sections from selected areas were contrasted with uranyl acetate and lead citrate and viewed with a Philips CM 100 electron microscope (Eindhoven, The Netherlands). At least five endplate regions were photographed from each muscle. Pictures were scanned for morphometric analysis using the ImageJ software. Analyzed parameters included the size of nerve boutons and the length of the presynaptic and postsynaptic membrane.[28,29]

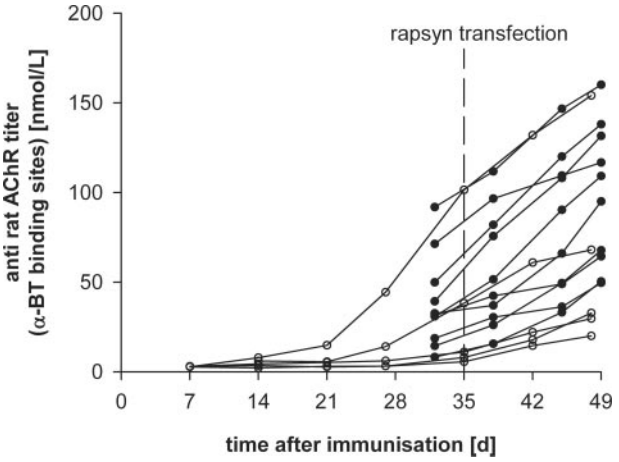

Figure 1. Time course of anti-rat AChR antibody titers in female Lewis rats immunized with 20 μg of *Torpedo* AChR in complete Freund's adjuvant at the age of 6 weeks (day 0). The tibialis anterior muscles were electroporated 5 weeks later and analyzed 7 weeks after immunization. Titers with **filled symbols** belong to animals used for the measurement of total AChR and AChR-antibody complexes in Figures 2 and 3. Titers with **open symbols** correspond to animals immunized for immunofluorescence studies shown in Figures 4 and 5.

Results

Rapsyn Overexpression Increases the Total Muscle AChR Concentration

Ten rats were immunized with tAChR, and five nonimmunized rats served as controls. All tAChR-immunized rats developed raised levels of antibodies to rat AChR 5 weeks later (Figure 1, black circles); these levels were comparable with those found in MG patients (data not shown). At this time point, the left tibialis anterior muscles of all animals were transfected with pcDNA-rapsyn by electropermeabilization (rapsyn-treated muscles). The right tibialis anterior muscles were electropermeabilized after injection of an equal volume of saline (untreated muscles). Two weeks after transfection, the animals were euthanized, and the concentration of total AChR (synaptic and extrasynaptic AChR) was subsequently measured by radioimmunoassay in muscle membrane extracts from individual tibialis anterior muscles.

The results are summarized in Figure 2A, and the correlation between AChR concentration and antibody titer is shown in Figure 2B. Similar to our previous re-

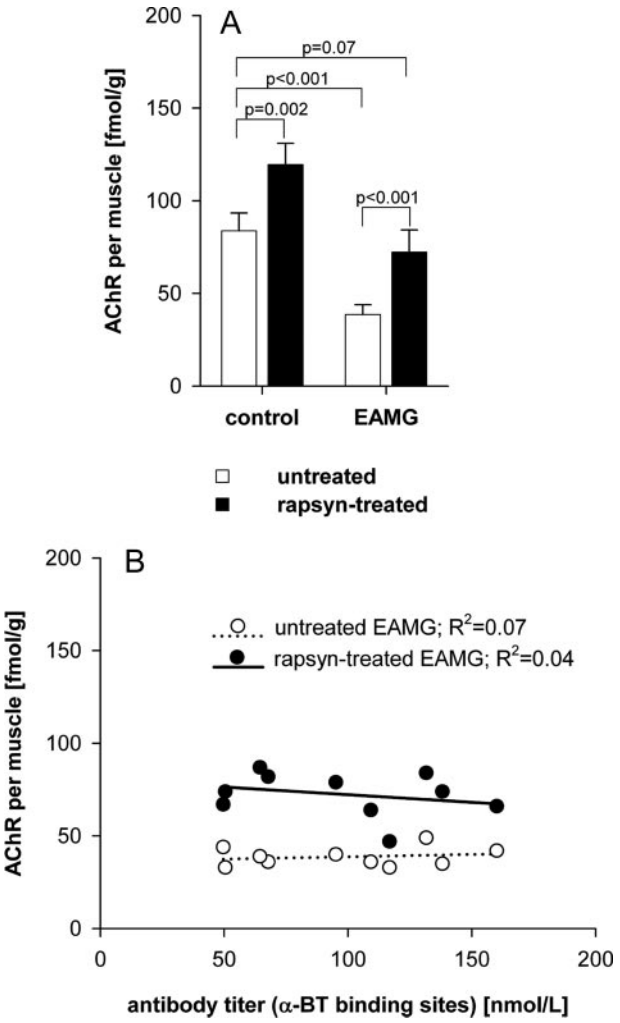

Figure 2. Effect of rapsyn overexpression on total membrane AChR concentration in control rats and in chronic EAMG rats. The AChR concentration of untreated and rapsyn-treated tibialis anterior muscles was measured in five control and 10 chronic EAMG rats by radioimmunoassay using ^{125}I-labeled α-BT. **A:** Average AChR concentration in the tibialis anterior muscles in untreated muscles (white bars) and rapsyn-treated muscles (black bars). **B:** The effect of anti-rat AChR antibody titer on AChR levels. **Open circles** indicate the total AChR of untreated muscles; **filled circles** correspond to total AChR of rapsyn-treated muscles. All rapsyn-treated muscles had an increased amount of total AChR compared with the untreated muscle of the same animal.

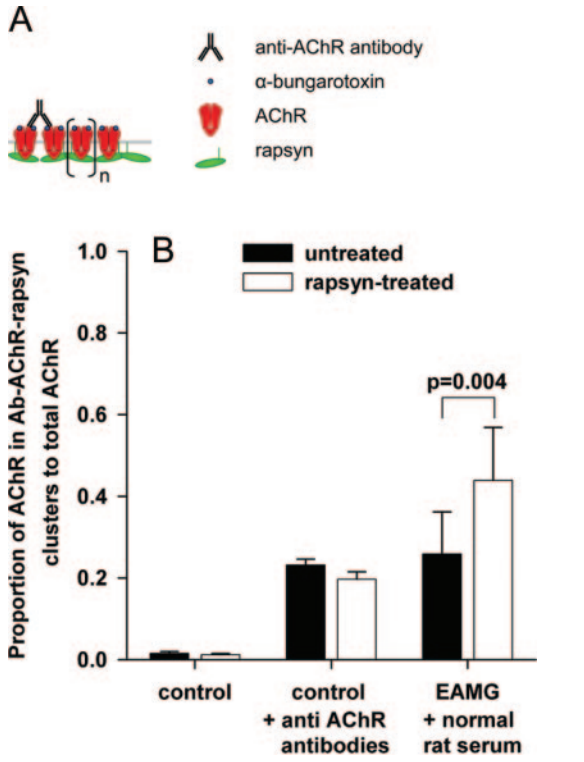

Figure 3. Measurement of antibody-AChR complexes and rapsyn-AChR aggregates by radioimmunoassay. AChR clustering by rapsyn was tested by adding a limited amount of anti-rat AChR antibody to membrane extracts of untreated and rapsyn-treated control muscles. **A:** Hypothetical scheme of AChR complexes, showing precipitation of AChR-rapsyn clusters by a limited amount of anti-AChR antibodies. Cross-linking of receptors by rapsyn (*n*) would lead to the co-precipitation of a larger amount of radioactive α-BT. If clustering by rapsyn is absent, more AChR remains in solution. **B:** Rapsyn transfection did not lead to increased size of rapsyn-AChR aggregates in membrane extracts of control muscles (control +AChR antibodies); cross-linking of AChR by rapsyn as shown in **A** did not occur. In EAMG muscles, rapsyn transfection resulted in increased *in vivo* binding of antibodies to AChR in EAMG animals (**B**, EAMG + normal rat serum).

sults,[18] rapsyn-treated muscles of control animals contained significantly more AChR than untreated muscles (an increase of 36 fmol/g, corresponding to 43%; $n = 5$; $P = 0.002$, paired *t*-test; Figure 2A, control). Electroporation of the empty vector did not change the AChR concentration compared with saline-treated muscles (data not shown).

Untreated EAMG muscles showed a significant reduction of AChR compared with untreated control muscles (−46%; $P < 0.001$, unpaired *t*-test) as expected, whereas the contralateral rapsyn-treated EAMG muscles showed an 87% increase in AChR compared with the untreated EAMG muscle (an increase of 34 fmol/g; $P < 0.001$, paired *t*-test; Figure 2A, EAMG). The AChR content of the rapsyn-treated EAMG muscles was similar to that in control untreated rat muscles (−14%; $P = 0.07$, unpaired *t*-test). As found in previous studies, there was no correlation between the antibody titer and the AChR loss of EAMG animals, either in the untreated or rapsyn-treated EAMG muscles (Figure 2B).

Rapsyn Overexpression Increases Antibody Binding to AChRs

Because rapsyn overexpression increased total AChR levels, we hypothesized that the AChR is metabolically stabilized in large rapsyn-AChR aggregates in the muscle membrane (Figure 3A). To see whether the rapsyn expression had led to aggregates of AChR, which could resist detergent extraction, we used limiting amounts of rat antiserum (64 fmol of α-BT-binding sites) to immunoprecipitate the AChRs from untreated and rapsyn-treated control muscle extracts. The rat antibodies were able to immunoprecipitate 23% of the total AChR in untreated control muscles and 20% in the rapsyn-treated control muscles (Figure 3B, control + anti-AChR antibodies). Thus, in normal animals rapsyn overexpression did not increase detergent soluble AChR aggregates; the hypo-

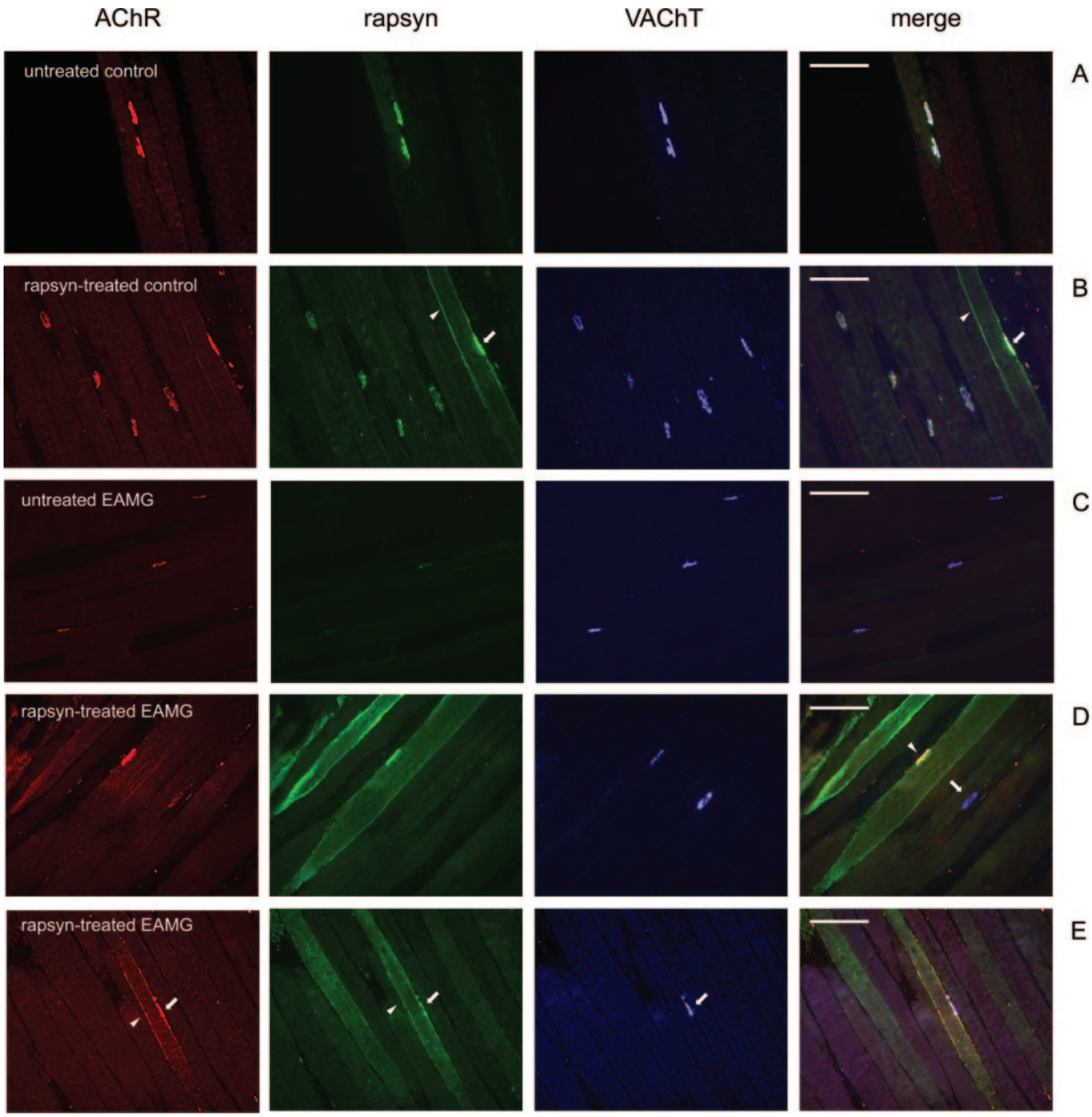

Figure 4. Cryosections of tibialis anterior muscles were triple-stained with Alexa 594-conjugated α-BT (red), mouse anti-rapsyn mAb1234 (green), and rabbit anti-VAChT (blue); merge on the right. **A:** In an untreated tibialis anterior muscle of a control rat AChR, rapsyn and VAChT are co-localized at the endplates. **B:** In the contralateral rapsyn-treated muscle of the same animal, rapsyn is localized extrasynaptically in the cell membrane of a transfected fiber (**arrowhead**). In this fiber, the endplate contains an increased amount of rapsyn (**arrow**). **C:** In untreated chronic EAMG muscles, endplates showed reduced staining of AChR and rapsyn but not VAChT. **D:** In rapsyn-treated EAMG muscles, the endplates in fibers with high amount of extrasynaptic rapsyn aggregates had a staining intensity of AChR and rapsyn that was similar to endplates of untreated control muscles (**arrowhead**). **D:** In other fibers without such aggregates, endplates had a reduced staining intensity for AChR and rapsyn (**arrow**). **E:** Extrasynaptic AChR co-localized with rapsyn (**arrowheads**) adjacent to the NMJ (**arrow**) in the membranes of transfected fibers. Scale bars = 100 μm.

thetical increase of AChR cross-linking by rapsyn (Figure 3A) was not observed in these membrane extracts.

In the EAMG rat muscles, immunoprecipitation of rat antibodies (in the presence of normal rat serum added as co-precipitant) indicated the proportion of AChRs with bound antibodies *in vivo*. The anti-AChR antibodies in the membrane extracts led to the precipitation of 26% of the AChR (Figure 3B, EAMG + normal rat serum) from untreated EAMG muscle. However, in the contralateral rapsyn-treated EAMG muscles 44% of the AChR was precipitated under the same conditions, indicating greater binding of antibody *in vivo* ($P = 0.004$, paired *t*-test).

Rapsyn Overexpression Increases the Amount of AChR and Rapsyn at Endplates and Extrasynaptic AChR Aggregates

To examine further the changes at the NMJ, we performed immunofluorescence studies in five EAMG and

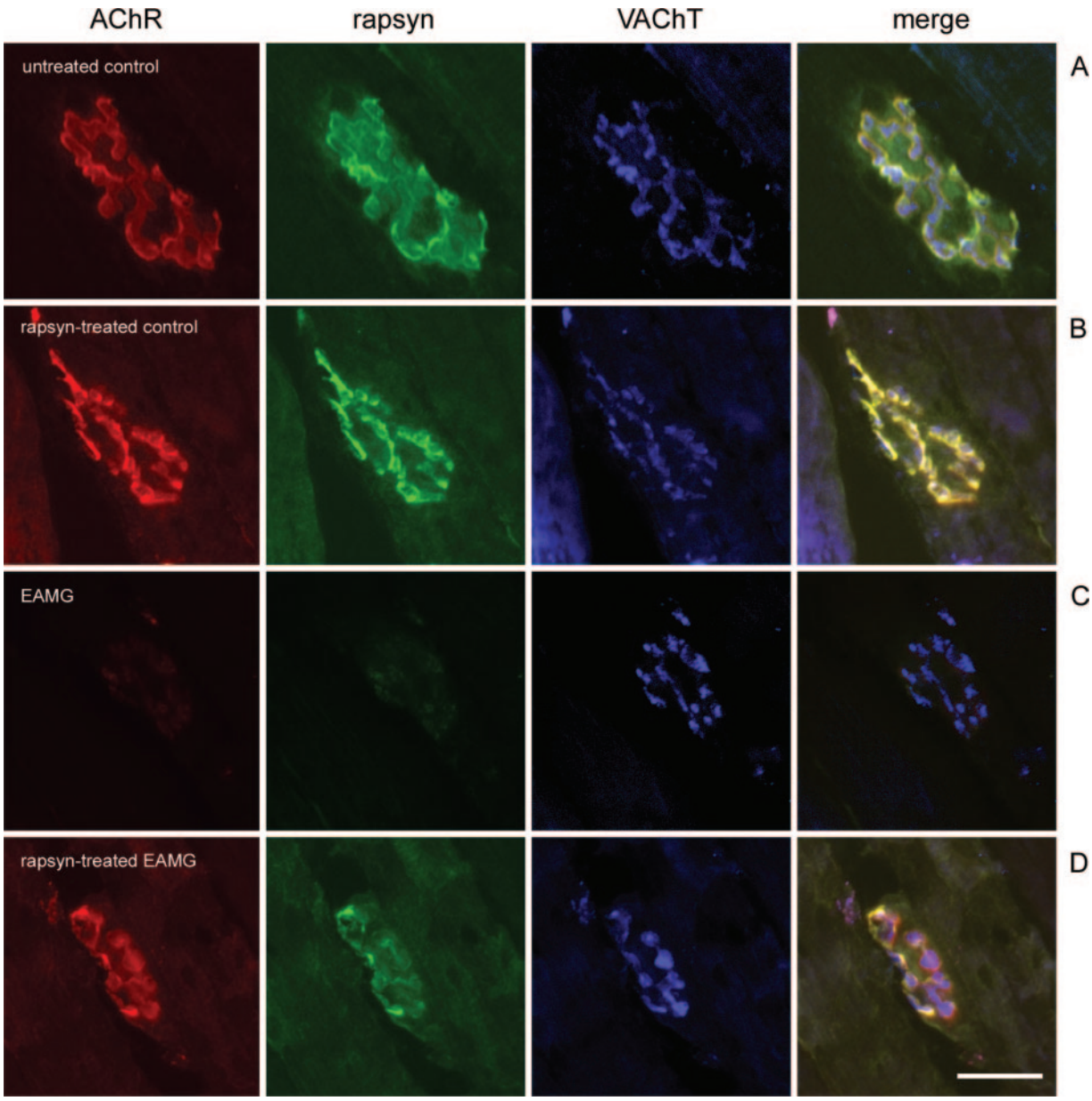

Figure 5. Immunohistochemical analysis of the NMJ using two-photon laser-scanning microscopy. AChR is stained red, rapsyn is stained green, and VAChT is stained blue; merge on the right. **A:** A normal endplate in an untreated control muscle shows co-localization of AChR and rapsyn in the postsynaptic membrane and the adjacent presynaptic VAChT staining. **B:** Rapsyn-treated endplate of a control animal. **C:** Endplate in an untreated EAMG muscle with reduced staining of AChR and rapsyn. **D:** Transfected endplate in a rapsyn-treated EAMG muscle with increased AChR and rapsyn. Scale bar = 20 μm.

three control rats. The immunized rats developed similar antibody titers (Figure 1, open circles) as in the previous experiment. The animals showed mild weakness after testing (grade +) with the exception of the animal with the highest antibody titer, which developed severe clinical symptoms (grade ++). Cryosections of the isolated tibialis anterior muscles were triple-stained for rapsyn, AChR, and VAChT, with results shown in Figures 4 and 5 and a quantitative summary in Figure 6.

In untreated muscles of control rats, AChR, rapsyn, and VAChT co-localized at the NMJs (Figure 4A) as expected. In addition, many muscle fibers from rapsyn-treated muscles of control rats had a large number of intensively stained extrasynaptic rapsyn aggregates of different sizes, localized in the cell membrane (Figure 4B) and in intracellular aggregates. Such aggregates in rapsyn-transfected fibers have been shown to correspond to Golgi-vesicles.[30]

In chronic EAMG rats, AChR and rapsyn staining of endplates of the untreated muscle was weak, relative to the presynaptic VAChT staining (Figure 4C). In the rapsyn-treated contralateral muscles, the endplates in fibers with intense staining of rapsyn also stained intensely for AChR (Figure 4D, endplate indicated with arrowhead). Endplates in fibers with a low amount of extrasynaptic rapsyn also stained weakly for AChR (Figure 4D, endplate indicated by arrow). A large number of extrasynaptic membrane rapsyn-AChR aggregates were

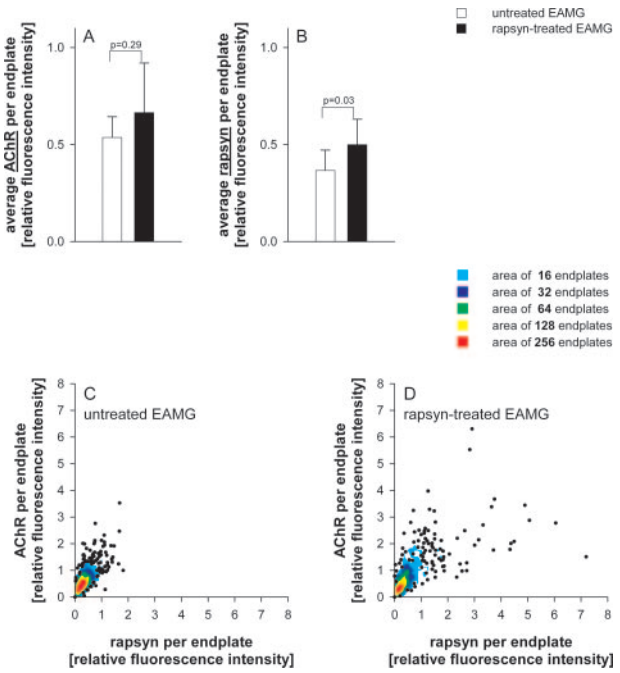

Figure 6. Measurement of fluorescence intensities of AChR and rapsyn relative to VAChT staining in untreated and rapsyn-treated muscles of five EAMG animals. At least 120 endplates were analyzed per muscle. Staining intensities were normalized to the average intensities of untreated control endplates. The average rapsyn staining was significantly increased at endplates of rapsyn-treated EAMG muscles compared with untreated muscles (**B**), but this did not lead to a significant increase of average synaptic AChR (**A**). The relative amount of AChR versus rapsyn in individual endplates are plotted in **C** for untreated EAMG animals and in **D** for the rapsyn-treated EAMG animals. Data points with great overlap were replaced by colored regions. The colors indicate the number of replaced points. In the rapsyn-treated muscles, ~10% of endplates had an increased amount of rapsyn (individual data points more than 2× normal rapsyn level in **D**, but only a few endplates had an increase of AChR compared with the endplates in untreated muscles).

found in rapsyn-treated muscles from EAMG rats (Figure 4E, arrowhead) but were absent in the contralateral untreated muscles (Figure 4C). By contrast, extrasynaptic rapsyn aggregates rarely co-localized with AChR in rapsyn-transfected muscle fibers of control rats (not shown).

We used two-photon confocal microscopy, at higher resolution, to examine the NMJs in more detail. Figure 5A shows a normal endplate in an untreated control muscle (frontal view). In this orientation, the projection shows postsynaptic co-localization of AChR and rapsyn as well as staining of VAChT in the adjacent nerve boutons. Figure 5B shows an endplate in a rapsyn-treated control muscle. No apparent structural differences were observed between endplates from untreated and rapsyn-treated control muscles. A representative endplate in an untreated EAMG muscle (Figure 5C) shows a normal VAChT staining but reduced amounts of rapsyn and AChR. In the rapsyn-treated EAMG muscles, only a small subset of NMJs showed increased AChR and rapsyn expression; most endplates were similar to untreated EAMG endplates. Even in highly rapsyn-transfected fibers, endplates only stained partly for rapsyn and AChR (Figure 5D).

To analyze the efficacy of rapsyn overexpression, the immunohistochemical staining of more than 200 endplates per tibialis anterior muscle were analyzed (Table 1). Postsynaptic AChR and rapsyn levels were measured relative to the presynaptic VAChT levels. The endplates of the untreated EAMG muscles showed a significant decrease of AChR and rapsyn staining compared with endplates from untreated control muscles: the average AChR staining was reduced by 46 ± 6% ($P < 0.001$, unpaired *t*-test), and rapsyn was reduced by 64% (±8%; $P < 0.001$, unpaired *t*-test). Endplates in the rapsyn-treated chronic EAMG muscles had slightly increased average staining of rapsyn (36%, $P = 0.03$, paired *t*-test; Figure 6B) and AChR (23%, $P = 0.29$, paired *t*-test; Figure 6A) compared with the contralateral untreated muscles. However, the rapsyn overexpression did not increase the average synaptic AChR and rapsyn to normal levels. The relative amount of AChR versus rapsyn in individual endplates is plotted in Figure 6C for untreated EAMG animals and in Figure 6D for the rapsyn-treated EAMG animals. Most endplates distribute closely around the average rapsyn and AChR levels in both conditions (red and yellow colored areas in Figure 6, C and D). Overall, only ~10% of all analyzed endplates in rapsyn-treated EAMG muscles had an increased synaptic rapsyn and AChR level (scattered individual points toward the top right in Figure 6D) compared with the contralateral untreated EAMG endplates.

Table 1. Quantification of Synaptic AChR and Rapsyn Relative to VAChT

Animal	Antibody titer (nmol/L)*	Untreated muscle		Rapsyn-treated muscle	
		AChR†	Rapsyn†	AChR†	Rapsyn†
1	20.0	0.84 ± 0.48 (n = 397)	0.51 ± 0.04 (n = 470)	0.63 ± 0.19	0.44 ± 0.10
2	29.6	0.56 ± 0.04 (n = 317)	0.37 ± 0.03 (n = 301)	1.10 ± 0.21	0.60 ± 0.2
3	32.8	0.71 ± 0.16 (n = 325)	0.41 ± 0.09 (n = 315)	0.69 ± 0.01	0.51 ± 0.43
4	68.1	0.46 ± 0.12 (n = 343)	0.37 ± 0.02 (n = 436)	0.53 ± 0.26	0.60 ± 0.45
5	154.0	0.45 ± 0.06 (n = 281)	0.20 ± 0.02 (n = 394)	0.51 ± 0.13	0.28 ± 0.08

*The antibody titer is represented as the equivalent of α-BT binding sites of precipitated AChR.
†The staining intensity of AChR and rapsyn was measured relative to presynaptic staining of VAChT. The results are normalized relative to average AChR and rapsyn levels of endplates in untreated control muscles. The values are the averages of two independent experiments (±SD) measuring protein levels in representative areas of the muscles. The number in parentheses is the total amount of endplates analyzed in both experiments.

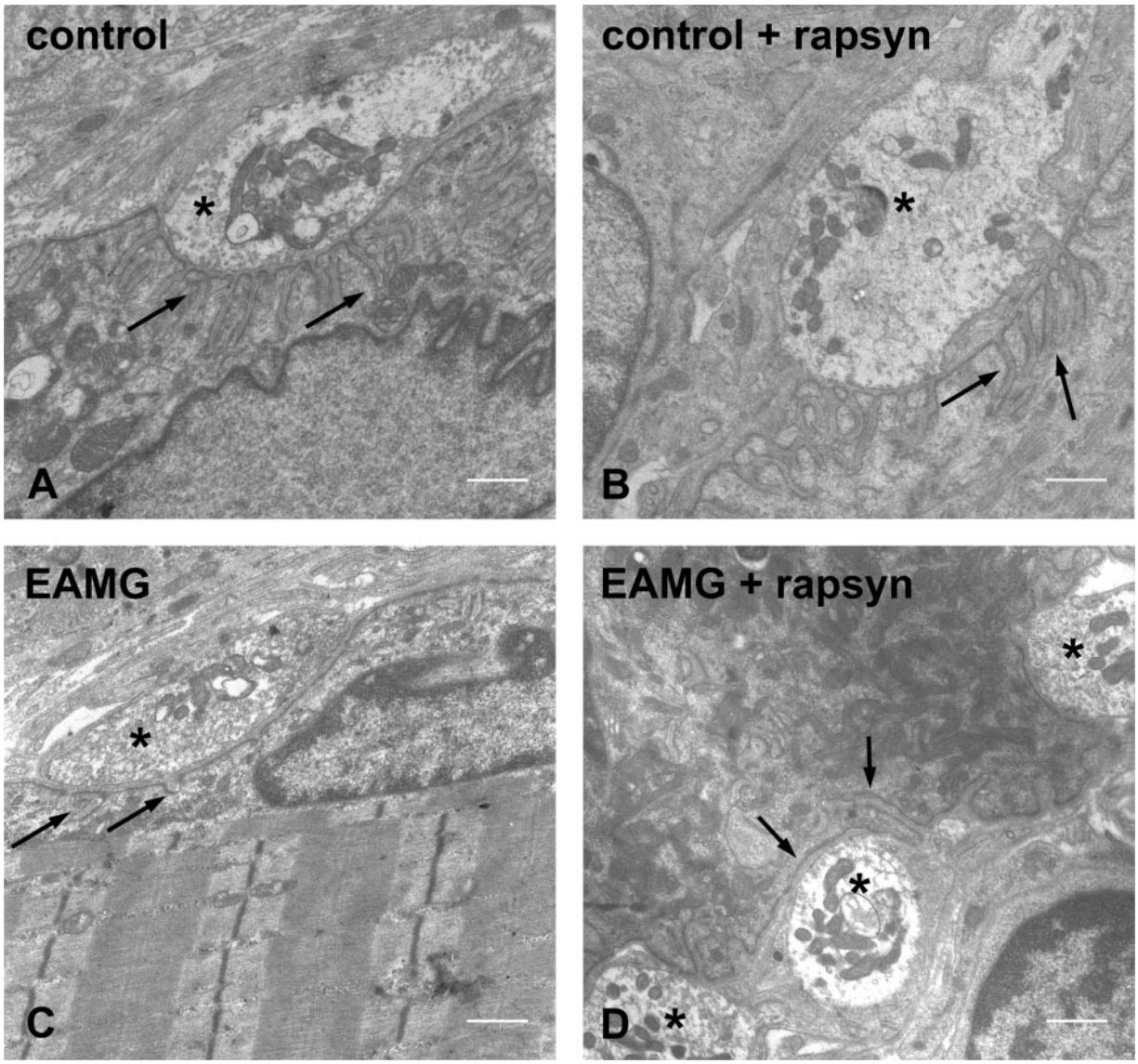

Figure 7. Electron microscopic examinations of the postsynaptic folds of motor endplates. NMJ in an untreated (**A**) and rapsyn-treated (**B**) tibialis anterior muscle. Damaged postsynaptic membrane without folds in an untreated tibialis anterior muscle (**C**) and in a rapsyn-treated tibialis anterior muscle (**D**) of an EAMG animal. **Arrows** indicate the postsynaptic membranes; **asterisks** indicate the nerve terminals. Scale bars = 1 μm.

Rapsyn Overexpression Does Not Prevent Complement Deposition at the NMJ

At all endplates of EAMG animals, the AChR co-localized with the membrane attack complex (not shown), consistent with a complement-dependent degradation of AChRs. Complement deposition was independent of rapsyn transfection. Therefore, the increased total AChR levels of rapsyn-transfected muscles cannot be explained by reduced complement activation. In control

Table 2. Morphometric Analysis of Endplates

	Regions analyzed*	Nerve bouton area (μm^2)	Presynaptic membrane length (μm)	Postsynaptic membrane length (μm)	Membrane length ratio (postsynaptic/ presynaptic)
Untreated control	76	5.9 ± 1.8	5.8 ± 1.8	24.7 ± 11.7	4.5 ± 0.9
Rapsyn-treated control	65	5.3 ± 2.6	4.9 ± 1.3	20.1 ± 7.8	4.0 ± 0.3
Untreated EAMG	57	5.0 ± 2.3	5.2 ± 1.1	12.7 ± 3.0†	2.5 ± 0.3†
Rapsyn-treated EAMG	24	6.9 ± 4.6	5.5 ± 1.7	8.1 ± 2.2‡	1.5 ± 0.02‡

Mean ± SD of three muscles for each condition.
*A region here refers to an area of one synaptic bouton and the adjacent postsynaptic membrane.
†Significantly different from untreated control endplates ($P < 0.05$) and significantly different from rapsyn-treated EAMG endplates ($P < 0.05$).
‡Significantly different from all other conditions ($P < 0.05$) and other differences in this table are not significant ($P > 0.05$).

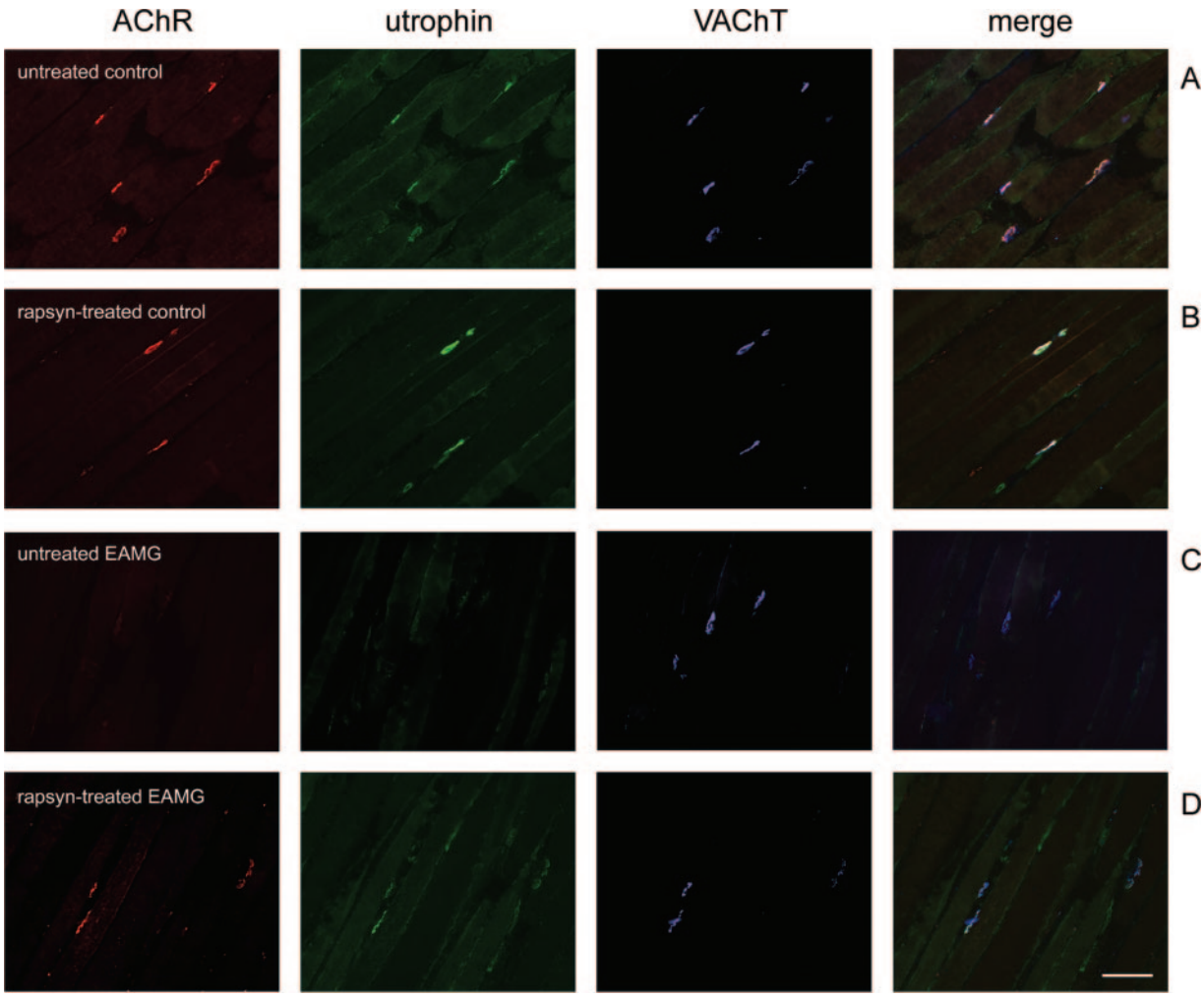

Figure 8. Cryosections of tibialis anterior muscles were stained with α-BT (red), mouse anti-utrophin mAb MANCHO 7 (green), and rabbit anti-VAChT (blue); merge on the right. **A** and **B:** In untreated and rapsyn-treated tibialis anterior muscles of a control rat, utrophin and VAChT are co-localized at the endplates. **C:** In chronic EAMG muscles, endplates showed reduced staining of utrophin but not VAChT. **D:** In rapsyn-treated EAMG muscles, the endplates with increased amount of AChR also stained intensively for utrophin. Scale bar = 100 μm.

muscles, membrane attack complex staining was absent as expected.

Rapsyn Overexpression Does Not Improve Neuromuscular Transmission in EAMG Rats

To study whether the increased amount of membrane AChR had an effect on neuromuscular transmission, we measured the compound muscle action potential on repetitive nerve stimulation in three control and three EAMG rats. In control rats, no decrement of the muscle compound action potential was found in untreated and rapsyn-treated muscles, even after injection of 3 or 6 μg of curare to sensitize neuromuscular transmission. In EAMG animals, no significant difference of the compound muscle action potential was found between untreated and rapsyn-treated muscles. Decrement was induced bilaterally in all EAMG rats by injection of 3 μg of curare.

Rapsyn Overexpression Reduces the Postsynaptic Membrane Length in EAMG Rats

To study, therefore, how the rapsyn overexpression affected the ultrastructure of the endplates in the rapsyn-treated EAMG muscles, we performed electron microscopic observations and morphometric analysis on three control and three EAMG rats. Rapsyn treatment did not appear to alter the structure of the NMJ in control muscles (Figure 7, A and B; and Table 2), which showed normal postsynaptic folds in all examined regions (76 endplate regions of untreated control muscles and 65 regions of rapsyn-treated control muscles). The postsynaptic membrane was severely damaged in untreated muscles of EAMG rats (Figure 7C) but even more so in the contralateral rapsyn-treated muscles (Figure 7D). In the untreated muscles of EAMG rats, all 57 endplate regions analyzed had reduced postsynaptic folds or even a complete loss of postsynaptic folding. The average length of the postsynaptic membrane was signifi-

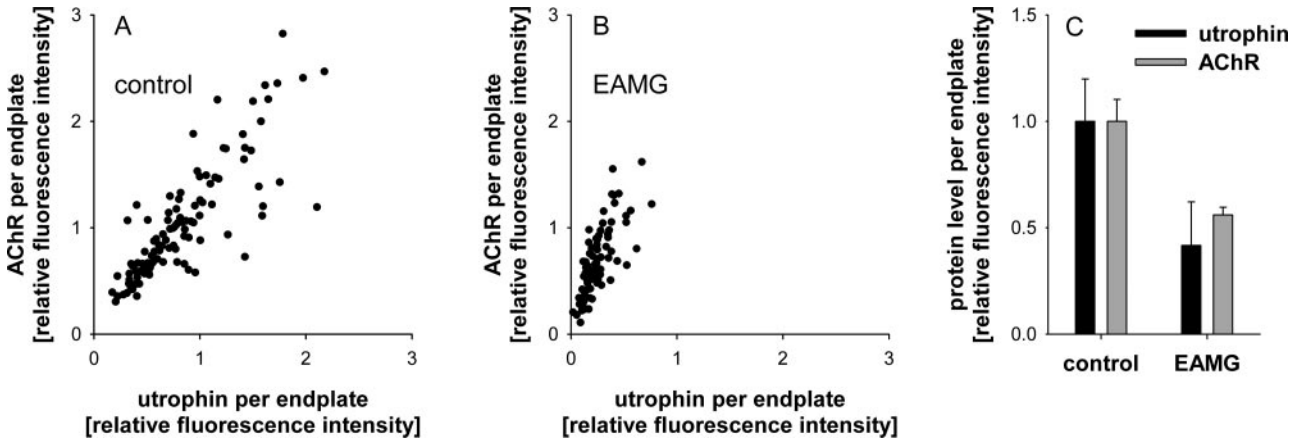

Figure 9. Measurement of fluorescence intensities of AChR and utrophin relative to VAChT staining. **A:** AChR levels correlate with utrophin levels in endplates of an untreated control muscle. **B:** In untreated EAMG muscles, AChR levels are significantly reduced. Utrophin levels are affected even stronger. **C:** Compared with untreated control endplates, the endplates in EAMG muscles have an average utrophin reduction of 58% and an average AChR reduction of 44%.

cantly reduced compared with normal endplates (Table 2). In the contralateral rapsyn-treated EAMG muscles, all 24 regions analyzed showed a complete destruction of the postsynaptic folding. The length of the postsynaptic membrane in rapsyn-treated endplates of EAMG rats was significantly shorter compared with the contralateral untreated muscles or to control muscles ($P < 0.05$, Table 2).

Utrophin Levels Are Reduced in Chronic EAMG Endplates

Because utrophin is involved in linking proteins of the NMJ to the cytoskeleton, we stained muscle sections of control and EAMG rats for utrophin and VAChT (Figure 8). Similar to the loss of rapsyn and AChR, utrophin staining was reduced in endplates of untreated EAMG muscles (Figure 8C). The average decrease of utrophin/VAChT in EAMG endplates was 58% compared with untreated control endplates (Figure 9). In endplates that stained intensely for AChR in rapsyn-treated EAMG muscles, the utrophin staining was also increased (Figure 8D). This suggests that utrophin contributes to the anchoring and stabilization of AChR-rapsyn aggregates to the cytoskeleton. This result also implies that increased rapsyn alone is not sufficient to recover the proteins of the damaged NMJ.

Discussion

Anti-AChR antibodies are the cause of the postsynaptic membrane destruction in most MG patients, but the anti-AChR antibody titer is not the only factor determining disease severity. Previous observations suggested that intrinsic differences in the expression of postsynaptic proteins are correlated to resistance to EAMG,[14] and we found that transfecting the AChR anchoring protein rapsyn alone is sufficient to prevent passively transferred disease in susceptible animals.[18] Here, we investigated the effect of rapsyn transfection in the chronic model of EAMG induced by active immunization. The results show an increase of total membrane AChR in rapsyn-transfected muscles of chronic EAMG animals, but the increased AChR was localized mainly extrasynaptically, rather than at the endplates, and was bound to antibodies. In concordance with these findings, at the ultrastructural level, most postsynaptic regions in rapsyn-treated muscles showed increased damage of the postsynaptic membrane, and the electrophysiological defects did not differ between treated and untreated muscles.

In rapsyn-treated muscles of control animals the amount of AChR was increased by 43% after 2 weeks, and the additional AChR was partly localized at endplates, as previously reported.[18] By immunohistochemistry, however, there were also extrasynaptic rapsyn-AChR aggregates in some fibers (schematically represented in Figure 10B), which were not present in the contralateral untreated muscles (Figure 10A). Rapsyn overexpression also increased the AChR levels in ongoing chronic EAMG. The total AChR concentration in rapsyn-treated EAMG muscles was increased by 87% compared with the contralateral untreated muscles, but significantly increased AChR levels were only found in ~10% of the endplates. Confocal microscopy observations were consistent with these results, showing that transfected fibers with high rapsyn expression near the endplate region had an increase of AChR levels at the endplate compared with untreated EAMG endplates but did not reach normal levels of AChR or even rapsyn in the entire endplate. It is possible that these endplates were not completely destroyed at the time of electroporation and were subsequently stabilized by the rapsyn transfection. A high number of extrasynaptic AChR-rapsyn aggregates were also found in these fibers. Therefore, the extrasynaptic aggregates account for most of the increased AChRs in these muscles (Figure 10D). Interestingly, a large proportion of the additional AChR was found to be complexed *in vivo* with antibodies, suggesting that rapsyn mediated the transport of extrasynaptic intracellular AChR to the cell membrane where it could bind the antibody. It is unlikely that this effect is caused by binding of circulating antibodies to epitopes of intracellular AChR because this phenomenon does not occur when isolated muscles are

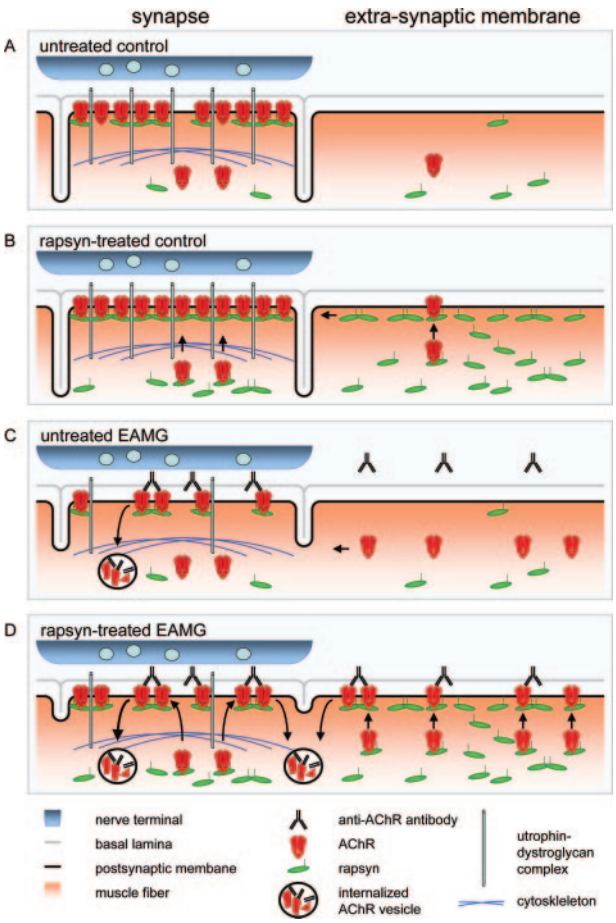

Figure 10. Schematic summary of the observed effects of rapsyn treatment in control and EAMG muscles. **A:** In untreated control muscles of young rats, the AChR is clustered densely but anchored incompletely to the cytoskeleton because of the low synaptic expression of rapsyn. Extrasynaptic rapsyn expression possibly contributes to the endplate maintenance (see Discussion). **B:** In rapsyn-treated controls, rapsyn anchors the AChR tightly to the cytoskeleton via the utrophin-dystroglycan complex. Extrasynaptic rapsyn accumulates in the cell membrane and is partially transported to the synapse. **C:** In untreated EAMG muscles, anti-AChR antibodies damage the postsynaptic membrane. AChR, rapsyn, and utrophin are degraded and the postsynaptic folding is reduced. Extrasynaptically, AChR is up-regulated as a consequence of functional denervation. The increased extrasynaptic AChR level helps to replace lost AChR at the endplate. **D:** In rapsyn-treated EAMG muscles, rapsyn and AChR co-localize both synaptically as well as extrasynaptically. Rapsyn increases the AChR clustering in the postsynaptic membrane, but the damage to the utrophin-dystroglycan complex prevents AChR anchoring to the cytoskeleton. Therefore, the newly clustered AChR is susceptible to antigenic modulation by antibodies and is internalized by endocytosis. The increased antibody binding and AChR turnover leads to an aggravation of the ultrastructural damage of the postsynaptic membrane. Moreover, extrasynaptic AChR clustering induced by rapsyn overexpression prevents AChR trafficking to the perisynaptic area and the replacement of lost AChR.

used for the muscle membrane extraction in contrast to total limb extraction.[27]

The analysis of immunohistochemical staining suggested that this extrasynaptic AChR and rapsyn were not relocated to the endplate, although there is accumulating evidence that these proteins can be actively transported individually to the NMJ after ectopic expression in transfected or transgenic muscle fibers.[30–33] It is likely that extrasynaptic aggregates of AChR and rapsyn that are complexed with autoantibodies cannot be transported and that this mechanism is responsible for the low levels of rapsyn and AChR observed at endplates of rapsyn-treated muscles and possibly also of untreated EAMG muscles. Trapping of AChR-rapsyn aggregates might aggravate the relatively low expression of rapsyn versus the AChR in EAMG.[34] The possibility that impaired rapsyn trafficking plays a role in EAMG is also supported by results of Kishi and colleagues,[35] who observed that rapsyn mRNA expression in normal muscle conditions is only increased 1.6× at the NMJ compared with other muscle areas, whereas other synaptic proteins reached up to 80-fold increased synaptic expression. Interestingly, the synaptic enrichment of rapsyn mRNA is age-dependent in rats,[36] thus paralleling the age-related resistance against EAMG.[14] Therefore, it will be interesting to study whether the enhancement of synaptic rapsyn expression helps to stabilize the AChR in EAMG more efficiently compared with the rapsyn expression in the whole muscle fiber.

The quantitative analysis of the ultrastructure showed that the increase of AChR and rapsyn levels in the muscle membrane of myasthenic rats had a detrimental effect on the postsynaptic folding. We found an increased binding of antibodies to AChR in rapsyn-transfected muscles, which can explain an accelerated complement-induced degradation of the postsynaptic membrane. This supports the hypothesis that rapsyn increases the clustering of AChR in the synaptic and extrasynaptic membrane and thereby making the AChR accessible to autoantibodies and inhibiting its trafficking to the NMJ from perisynaptic areas.[37] It has been suggested that the reduced AChR density after passive transfer EAMG limits further damage to the postsynaptic membrane after subsequent immunization with anti-AChR antibodies.[38] Our results are compatible with this mechanism and indicate that increased expression of AChR and rapsyn in ongoing EAMG enhances antibody binding and membrane damage.

Consequently, rapsyn alone is not sufficient to anchor the AChR efficiently in the membrane when the NMJ is already damaged. We observed that apart from the AChR and rapsyn, utrophin levels are also reduced in chronic EAMG. Loss of utrophin has also been reported for endplates of MG patients with anti-AChR antibodies.[39,40] The loss of utrophin and possibly other proteins of the dystrophin-glycoprotein complex at the NMJ (Figure 10C) might restrict the anchoring of AChR-rapsyn clusters to the cytoskeleton (Figure 10D). The difficulty to restore the NMJ structure is illustrated by the fact that in passive transfer EAMG the postsynaptic membrane is still significantly reduced 54 days after injection of anti-AChR antibodies.[41] In chronic EAMG, the postsynaptic membrane is continuously degraded, and its proteins have to be continuously replaced. Up-regulation of rapsyn increases the AChR concentration in the disease, but this AChR is not sufficiently stabilized at the endplate. Therefore, a better understanding of rapsyn interaction with other proteins in the NMJ may reveal new factors that can modulate the clinical severity in myasthenia gravis. Taken together, our data help to understand the role of rapsyn in the disease and indicate that, as a possible treatment of chronic EAMG muscles, rapsyn overexpres-

sion has to be targeted specifically to the endplate region and requires other postsynaptic proteins, including utrophin, for anchoring the AChR. Moreover, the results presented here show that rapsyn expression determines the susceptibility to EAMG and possibly MG in a complex way: high rapsyn expression anchors the AChR and prevents antibody- and complement-induced damage to the postsynaptic membrane, but when postsynaptic membrane is already damaged, high rapsyn expression increases membrane damage.

Acknowledgments

We thank M. van Zandvoort and W. Engels (Department of Biophysics, Universiteit Maastricht, Maastricht, The Netherlands) for their help with two-photon confocal microscopy; and M.V. Waarenburg, B. Machiels, and H.P.J. Steinbusch for their excellent technical assistance.

References

1. Sanes JR, Lichtman JW: Development of the vertebrate neuromuscular junction. Annu Rev Neurosci 1999, 22:389–442
2. De Baets M, Stassen MH: The role of antibodies in myasthenia gravis. J Neurol Sci 2002, 202:5–11
3. Gautam M, Noakes PG, Mudd J, Nichol M, Chu GC, Sanes JR, Merlie JP: Failure of postsynaptic specialization to develop at neuromuscular junctions of rapsyn-deficient mice. Nature 1995, 377:232–236
4. Glass DJ, Bowen DC, Stitt TN, Radziejewski C, Bruno J, Ryan TE, Gies DR, Shah S, Mattsson K, Burden SJ, DiStefano PS, Valenzuela DM, DeChiara TM, Yancopoulos GD: Agrin acts via a MuSK receptor complex. Cell 1996, 85:513–523
5. Moransard M, Borges LS, Willmann R, Marangi PA, Brenner HR, Ferns MJ, Fuhrer C: Agrin regulates rapsyn interaction with surface acetylcholine receptors, and this underlies cytoskeletal anchoring and clustering. J Biol Chem 2003, 278:7350–7359
6. Cartaud A, Coutant S, Petrucci TC, Cartaud J: Evidence for in situ and in vitro association between beta-dystroglycan and the subsynaptic 43K rapsyn protein. Consequence for acetylcholine receptor clustering at the synapse. J Biol Chem 1998, 273:11321–11326
7. Rybakova IN, Humston JL, Sonnemann KJ, Ervasti JM: Dystrophin and utrophin bind actin through distinct modes of contact. J Biol Chem 2006, 281:9996–10001
8. Ohno K, Engel AG, Shen XM, Selcen D, Brengman J, Harper CM, Tsujino A, Milone M: Rapsyn mutations in humans cause endplate acetylcholine-receptor deficiency and myasthenic syndrome. Am J Hum Genet 2002, 70:875–885
9. Ohno K, Sadeh M, Blatt I, Brengman JM, Engel AG: E-box mutations in the RAPSN promoter region in eight cases with congenital myasthenic syndrome. Hum Mol Genet 2003, 12:739–748
10. Phillips WD, Vladeta D, Han H, Noakes PG: Rapsyn and agrin slow the metabolic degradation of the acetylcholine receptor. Mol Cell Neurosci 1997, 10:16–26
11. Wang ZZ, Mathias A, Gautam M, Hall ZW: Metabolic stabilization of muscle nicotinic acetylcholine receptor by rapsyn. J Neurosci 1999, 19:1998–2007
12. Lennon VA, Lindstrom JM, Seybold ME: Experimental autoimmune myasthenia: a model of myasthenia gravis in rats and guinea pigs. J Exp Med 1975, 141:1365–1375
13. Graus YM, Verschuuren JJ, Spaans F, Jennekens F, van Breda Vriesman PJ, De Baets MH: Age-related resistance to experimental autoimmune myasthenia gravis in rats. J Immunol 1993, 150:4093–4103
14. Hoedemaekers A, Bessereau JL, Graus Y, Guyon T, Changeux JP, Berrih-Aknin S, van Breda Vriesman P, De Baets MH: Role of the target organ in determining susceptibility to experimental autoimmune myasthenia gravis. J Neuroimmunol 1998, 89:131–141
15. Hoedemaekers A, Graus Y, van Breda Vriesman P, de Baets M: Age- and sex-related resistance to chronic experimental autoimmune myasthenia gravis (EAMG) in Brown Norway rats. Clin Exp Immunol 1997, 107:189–197
16. Hoedemaekers A, Verschuuren JJ, Spaans F, Graus YF, Riemersma S, van Breda Vriesman PJ, De Baets MH: Age-related susceptibility to experimental autoimmune myasthenia gravis: immunological and electrophysiological aspects. Muscle Nerve 1997, 20:1091–1101
17. Hoedemaekers A, Graus Y, Beijleveld L, van Breda Vriesman P, De Baets M: Macrophage infiltration at the neuromuscular junction does not contribute to AChR loss and age-related resistance to EAMG. J Neuroimmunol 1997, 75:147–155
18. Losen M, Stassen MH, Martinez-Martinez P, Machiels BM, Duimel H, Frederik P, Veldman H, Wokke JH, Spaans F, Vincent A, De Baets MH: Increased expression of rapsyn in muscles prevents acetylcholine receptor loss in experimental autoimmune myasthenia gravis. Brain 2005, 128:2327–2337
19. Mir LM, Bureau MF, Gehl J, Rangara R, Rouy D, Caillaud JM, Delaere P, Branellec D, Schwartz B, Scherman D: High-efficiency gene transfer into skeletal muscle mediated by electric pulses. Proc Natl Acad Sci USA 1999, 96:4262–4267
20. Verschuuren JJ, Spaans F, De Baets MH: Single-fiber electromyography in experimental autoimmune myasthenia gravis. Muscle Nerve 1990, 13:485–492
21. Seybold ME, Lambert EH, Lennon VA, Lindstrom JM: Experimental autoimmune myasthenia: clinical, neurophysiologic, and pharmacologic aspects. Ann NY Acad Sci 1976, 274:275–282
22. Kimura J: Electrodiagnosis in Diseases of Nerve and Muscle: Principles and Practice. Oxford, Oxford University Press, 2001, p 1024
23. Bloch RJ, Froehner SC: The relationship of the postsynaptic 43K protein to acetylcholine receptors in receptor clusters isolated from cultured rat myotubes. J Cell Biol 1987, 104:645–654
24. Nguyen T, Ellis J, Love D, Davies K, Gatter K, Dickson G, Morris G: Localization of the DMDL gene-encoded dystrophin-related protein using a panel of nineteen monoclonal antibodies: presence at neuromuscular junctions, in the sarcolemma of dystrophic skeletal muscle, in vascular and other smooth muscles, and in proliferating brain cell lines. J Cell Biol 1991, 115:1695–1700
25. van Zandvoort M, Engels W, Douma K, Beckers L, Oude Egbrink M, Daemen M, Slaaf DW: Two-photon microscopy for imaging of the (atherosclerotic) vascular wall: a proof of concept study. J Vasc Res 2004, 41:54–63
26. Lindstrom JM, Lennon VA, Seybold ME, Whittingham S: Experimental autoimmune myasthenia gravis and myasthenia gravis: biochemical and immunochemical aspects. Ann NY Acad Sci 1976, 274:254–274
27. Verschuuren JJ, Graus YM, Theunissen RO, Yamamoto T, Vincent A, van Breda Vriesman PJ, De Baets MH: Role of acetylcholine receptor antibody complexes in muscle in experimental autoimmune myasthenia gravis. J Neuroimmunol 1992, 36:117–125
28. Engel AG, Tsujihata M, Lambert EH, Lindstrom JM, Lennon VA: Experimental autoimmune myasthenia gravis: a sequential and quantitative study of the neuromuscular junction ultrastructure and electrophysiologic correlations. J Neuropathol Exp Neurol 1976, 35:569–587
29. Engel AG, Tsujihata M, Lindstrom JM, Lennon VA: The motor end plate in myasthenia gravis and in experimental autoimmune myasthenia gravis. A quantitative ultrastructural study. Ann NY Acad Sci 1976, 274:60–79
30. Gervásio OL, Phillips WD: Increased ratio of rapsyn to ACh receptor stabilizes postsynaptic receptors at the mouse neuromuscular synapse. J Physiol 2005, 562:673–685
31. Gensler S, Sander A, Korngreen A, Traina G, Giese G, Witzemann V: Assembly and clustering of acetylcholine receptors containing GFP-tagged epsilon or gamma subunits: selective targeting to the neuromuscular junction in vivo. Eur J Biochem 2001, 268:2209–2217
32. Marangi PA, Forsayeth JR, Mittaud P, Erb-Vogtli S, Blake DJ, Moransard M, Sander A, Fuhrer C: Acetylcholine receptors are required for agrin-induced clustering of postsynaptic proteins. EMBO J 2001, 20:7060–7073
33. Ono F, Mandel G, Brehm P: Acetylcholine receptors direct rapsyn clusters to the neuromuscular synapse in zebrafish. J Neurosci 2004, 24:5475–5481
34. Asher O, Kues WA, Witzemann V, Tzartos SJ, Fuchs S, Souroujon MC:

Increased gene expression of acetylcholine receptor and myogenic factors in passively transferred experimental autoimmune myasthenia gravis. J Immunol 1993, 151:6442–6450
35. Kishi M, Kummer TT, Eglen SJ, Sanes JR: LL5beta: a regulator of postsynaptic differentiation identified in a screen for synaptically enriched transcripts at the neuromuscular junction. J Cell Biol 2005, 169:355–366
36. Moscoso LM, Merlie JP, Sanes JR: N-CAM, 43K-rapsyn, and S-laminin mRNAs are concentrated at synaptic sites in muscle fibers. Mol Cell Neurosci 1995, 6:80–89
37. Akaaboune M, Culican SM, Turney SG, Lichtman JW: Rapid and reversible effects of activity on acetylcholine receptor density at the neuromuscular junction in vivo. Science 1999, 286:503–507
38. Corey AL, Richman DP, Agius MA, Wollmann RL: Refractoriness to a second episode of experimental myasthenia gravis. Correlation with AChR concentration and morphologic appearance of the postsynaptic membrane. J Immunol 1987, 138:3269–3275
39. Ito H, Yoshimura T, Satoh A, Takino H, Tsujihata M, Nagataki S: Immunohistochemical study of utrophin and dystrophin at the motor end-plate in myasthenia gravis. Acta Neuropathol (Berl) 1996, 92:14–18
40. Slater CR, Young C, Wood SJ, Bewick GS, Anderson LV, Baxter P, Fawcett PR, Roberts M, Jacobson L, Kuks J, Vincent A, Newsom-Davis J: Utrophin abundance is reduced at neuromuscular junctions of patients with both inherited and acquired acetylcholine receptor deficiencies. Brain 1997, 120:1513–1531
41. Engel AG, Sakakibara H, Sahashi K, Lindstrom JM, Lambert EH, Lennon VA: Passively transferred experimental autoimmune myasthenia gravis. Sequential and quantitative study of the motor end-plate fine structure and ultrastructural localization of immune complexes (IgG and C3), and of the acetylcholine receptor. Neurology 1979, 29:179–188